Pacific Northwest NATIONAL LABORATORY

PNNL-34701

Aggregation of Inverter-based Resources for Modelling and Simulation

August 23, 2023

Xue Lyu
Jing Xie
Thomas McDermott

U.S. DEPARTMENT OF ENERGY

Prepared for the U.S. Department of Energy
under Contract DE-AC05-76RL01830

PACIFIC NORTHWEST NATIONAL LABORATORY
operated by
BATTELLE
for the
UNITED STATES DEPARTMENT OF ENERGY
under Contract DE-AC05-76RL01830

Printed in the United States of America

Available to DOE and DOE contractors from
the Office of Scientific and Technical Information,
P.O. Box 62, Oak Ridge, TN 37831-0062
www.osti.gov
ph: (865) 576-8401
fox: (865) 576-5728
email: reports@osti.gov

Available to the public from the National Technical Information Service
5301 Shawnee Rd., Alexandria, VA 22312
ph: (800) 553-NTIS (6847)
or (703) 605-6000
email: info@ntis.gov
Online ordering: http://www.ntis.gov

PNNL-34701

Aggregation of Inverter-based Resources for Modelling and Simulation

August 23, 2023

Xue Lyu
Jing Xie
Thomas McDermott

Prepared for
Essential Grid Operations for Solar (EOS) Project

Pacific Northwest National Laboratory
Richland, Washington 99354

Aggregation of Inverter-Based Resources for Modeling and Simulation

Xue Lyu, Jing Xie, Thomas E. McDermott

Pacific Northwest National Laboratory

August 23, 2023

1 Motivation

The installed capacity of inverter-based resources (IBRs), e.g., battery energy storage system (BESS), wind, and solar photovoltaic (PV) systems is steadily increasing [1]. As IBRs are typically connected to the power grid using numerous paralleled inverters, several differential equations are required for modeling and simulation. The large-scale integration of IBRs poses challenges on the studies of steady state, dynamic, transient, and sub-transit response, since the rapidly expanding number of inverters increases both system order and complexity [2].

In order to conduct system dynamic studies, it is necessary to have dynamic models of both inverter and plant levels. Detailed and aggregated modeling approaches are two essential options. The detailed modeling method involves capturing the dynamic characteristics of each individual device (e.g., wind turbine or PV array), as well as their interconnections. However, as the scale of the IBR plant increases, the complexity and computation time required for detailed modeling also increase. On the other hand, aggregated modeling offers a more efficient way of representing large-scale IBRs in power system dynamic studies. This approach involves aggregating a large number of wind turbines, PV arrays, inverters, and/or plant controllers into one or a smaller number of equivalent models. In order to analyze the impact of a high-level IBR penetration in power systems, it is important to develop accurate and computationally efficient models for both the detailed and aggregated methods.

2 Existing Methods

Some aggregation modelling methods are proposed in existing works. In [3], an aggregated PV power plant that formed by string inverters-inverters is proposed through block aggregation in low-voltage (LV). This aggregation method groups the inverters and lines of the LV side per each medium voltage (MV) transformer.

A general method to derive an equivalent model of a large-scale PV power plant using a controller that embeds converters with synchronous dynamics is presented in [4] with the objective of reproducing the active and reactive power response at the point of connection of the plant while reducing the computation time. A distribution-network-cognizant aggregation approach that describes the collective dynamics of grid-tied three-phase inverters is developed in [5]. Inverters are clustered based on effective electrical distances to the feederhead in this work, and for each cluster, the developed aggregate dynamical model preserves the structure and order of each individual inverter state-space model. A weighted dynamic aggregation model for grid-following inverters and their controllers are proposed in [6]. The weight of each inverter is determined based on the contribution of each unit to the desired state dynamic behavior in the system.

3 Applications

The aggregation methods previously discussed are applicable to various scenarios. The selection of an appropriate model is contingent upon the operating conditions of the power plant and the specific objectives of the analysis. A comparison of those four methods is reported in Table 1. Details are also discussed as follows.

Methods	**PV Farm**	**Wind Farm**	**BESS**	**Complexity**	**RMS**	**EMT**
Block aggregation in LV	$\surd$	$\surd$	$\surd$	Low	$\surd$	$\times$
Equivalent model aggregation	$\surd$	$\surd$	$\surd$	Low	$\surd$	$\times$
Dynamic aggregation	$\surd$	$\surd$	$\surd$	High	$\surd$	$\surd$
Weighted dynamic aggregation	$\surd$	$\times$	$\times$	High	$\surd$	$\surd$

Table 1: Comparison of different methods.

The aggregation method in [3] uses an aggregated Electricity Generation Modules, 'Módulos de Generación de Electricidad' (MGE) simulation model of a PV power plant to conduct the complementary simulations required to obtain the final MGE certificate. Compared with other method, this one is easy to implement. According to this work, the fault ride through (FRT) capability of the power plant, that need to be complied with at power plant level, but which, nevertheless, may be certified at Power Generation Units, 'Unidades de Generaci ón de Electricidad' (UGE). As a result, the proposed aggregated model can be used to assess power plant compliance with power-frequency requirements, but it cannot be used to check whether the power plant meets the FRT requirements. The aggregation method is tested in an actual PV power plant with 42 MW nominal power formed by 465 inverters located in Spain. the use of an aggregated Electricity Generation Modules, 'Módulos de Generación de Electricidad (MGE) simulation model of a PV power plant -instead of a detailed MGE simulation model- to conduct the complementary simulations required to obtain the final MGE certificate when following the equipment certification path

The method in [4] is applicable to a solar or wind power plant that the inverters in the plant are controlled by a synchronous power controller. The equivalent model can reproduce a similar behavior of the active and reactive power exchanged between the grid and the power plant at its point of interconnection (POI). Hence the derived model is for root mean square (RMS) analysis not for electromagnetic transient (EMT) anaylysis. The proposed model is tested in a 100 MW PV power plant with 100 power conversion units. In particular, the internal network in the tested PV plant is formed by five rings, and each ring is aggregated via the proposed equivalent model.

The model-reduction method proposed in [5] is applicable to networks of inverters with different power ratings and reference power set-points and connect to an arbitrary network topology. The structure and order of each individual inverter state-space model can be reserved in the proposed model. It can be used to capture the impact of fast variations in irradiance on the output power of PV systems, modeling the impact of wind gusts on the output power of wind energy conversion systems, and uncovering the impact of changing set-points of large collections of inverters by aggregators (for frequency regulation or other grid services) on their collective outputs. This model-reduction method is validated in a modified IEEE 37-bus network with 15 inverters.

The weighted dynamic aggregation model proposed in [6] can be used to mimic the steady-state, transient, and dynamic behavior of the system, and it can also be used to design the controller and inverter parameters to ensure desirable performance of the large-scale system. The aggregation method can find an equivalent set of dynamic equations with a similar structure of a single PV unit to represent the PV farm. A small-scale system that consists three PV units is used to verify the accuracy of the proposed method. A CIGRE HV/MV 14-bus benchmark is used to verify the functionality of the proposed method in a large-scale system.

4 Case Studies

This section presents the test system, configurations, and simulation results of two scenarios. The effectiveness of the aggregated solar farm models is further analysed and discussed.

4.1 Test System

A 50 MW grid-connected solar PV plant is modelled in Simulink [7] and the model is modified according to [8]. System configurations are shown in Fig. 1 and Fig. 2, respectively. In Fig. 1, the PV plant is represented via a lumped inverter. This inverter is connected to the power system through an inductor–capacitor (LC) filter and a transformer. In Fig. 2, the PV plant is represented via four inverters, where each of them has a nominal power of 12.5 MW. The inverter is modeled using a pulse width modulation (PWM) controlled 3-level insulated-gate bipolar transistor (IGBT) bridge. It operates at a standard grid-following (GFL) control mode. The control system includes Maximum Power Point Tracking (MPPT) controller, V_{dc} regulator, current regulator, phase locked loop (PLL)(a three-phase PLL based on the synchronous reference frame is used in this work [9]) and PWM generator. The MPPT controller is based on the Perturb and Observe (P&O) technique [10]. The V_{dc} regulator determines the required I_d (active current) reference for the current regulator. The current regulator determines the required reference voltages for the inverter based on the current reference I_d and I_q. In this case, the I_q reference is set to zero. The PLL is for synchronization. PWM generator generates firing signals to the IGBTs based on the required reference voltages.

Assuming that the base power of the test system in Fig. 1 is 50 MW and the base voltage is 25 kV. For the test system in Fig. 2, assuming that the base power is 12.5 MW and the base voltage is 25 kV. The nominal frequency $F_{\mathrm{nom}} = 60$ Hz. The carrier frequency of the PWM modulator is $F_{\mathrm{c}} = 1980$ Hz. The step size of EMT simulation in Simulink is 5.0505 μs (i.e., $\frac{1}{100F_{\mathrm{c}}}$). Measurements are exported with a step size of 0.05 s for plotting purposes. This allows for a reduction in data size during processing, while still ensuring accurate and meaningful figures.

The parameters of the PV farm are shown in Table 2, where $N^1_{\mathrm{par}}, N^1_{\mathrm{ser}}$ are the parallel string PV modules and series-connected modules per string of 1-cluster of PV model, $N^4_{\mathrm{par}}, N^4_{\mathrm{ser}}$ are the same parameters of 4-clusters of PV model, X_L is the filter reactance, R_l is the filter resistance, C_f is the filter capacitance, R_1 is the transformer resistance, and L_1 is the transformer leakage inductance.

$\mathbf{N^1_{par}}$	$\mathbf{N^1_{ser}}$	$\mathbf{N^4_{par}}$	$\mathbf{N^4_{ser}}$	$\mathbf{X_L}$	$\mathbf{R_L}$	$\mathbf{C_f}$	$\mathbf{R_1}$	$\mathbf{L_1}$
880	140	220	140	0.15 p.u.	0.0015 p.u.	0.1 p.u.	0.0012 p.u.	0.03 p.u.

Table 2: Parameter of the test system.

4.2 Scenario 1 - Variations in Irradiance

Scenario 1 considers the normal operation with irradiance changes. The irradiance, the total active power of the PV plant, the DC voltage of the inverter, the AC voltage at the 25 kV bus, the frequency of the 25 kV bus are given in Fig. 3. When using the P&O method to generate the DC voltage reference

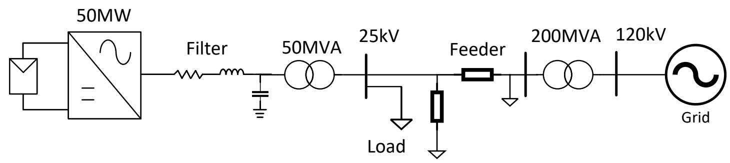

Figure 1: Tested system with 1-cluster of PV model.

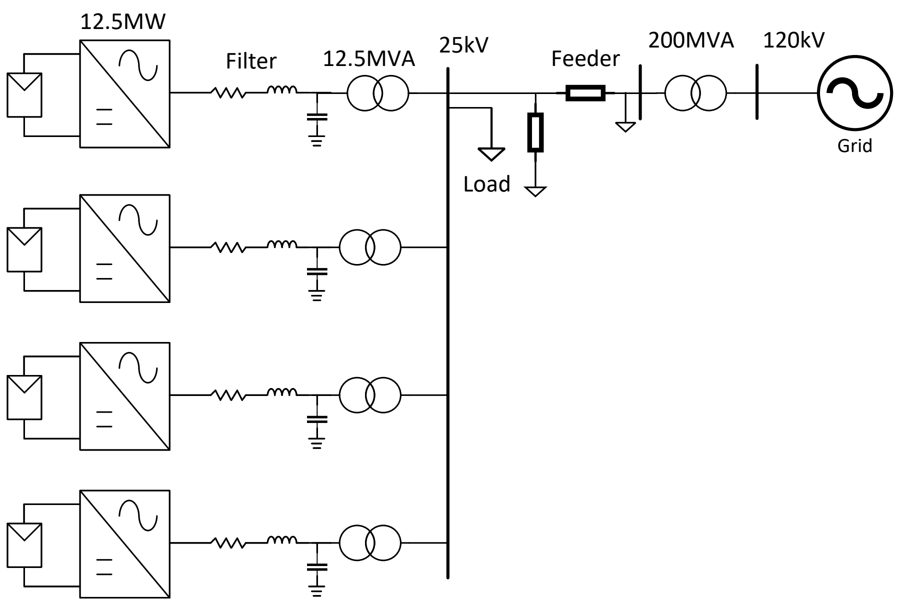

Figure 2: Tested system with 4-cluster of PV model.

for extracting the maximum available solar power, a minor distinction arises between these two modelling methods. Consequently, the measured DC voltage of the PV array in these two models exhibits a slight discrepancy. This variance further impacts the active power injected into the grid by the solar farm, subsequently resulting in a frequency difference that is measured at the POI, specifically at the 25 kV bus. The reactive power of the solar farm using these two modelling methods also exhibits a minor difference, resulting in a variance in the voltage magnitude at the 25 kV bus. According to Fig. 3, when sudden decreases and increases in irradiance occur, the simulation results of the solar farm using these two modeling methods also exhibit a strong agreement. Overall, the disparity in the simulation results between these two aggregation methods is marginal and falls within acceptable limits for typical analysis.

4.3 Scenario 2 - Fault Condition

In this scenario, the fault condition is tested. A single-phase bolted fault is applied to the system at 3 sec at the 25 kV bus, with the fault duration set to 300 ms. The irradiance remains constant at 1000 W/m^2 throughout the simulation. As demonstrated in Fig. 4, the difference between the DC voltage, the total re/active power of the solar farm, the frequency and voltage magnitude of the 25 kV bus during voltage fault with these two modelling strategies is small, which verifies that this type of aggregation strategy is applicable for the fault study.

4.4 Simulation time

Regarding simulation time, the utilization of the 1-cluster model results in a substantial reduction of 64% compared to the 4-cluster model. This outcome reasonably leads to the deduction that adopting the aggregated model will lead to a significant reduction in computational time.

5 Conclusion

This report briefly discusses different aggregation modeling methods for the integration of IBRs in power systems. In general, there is a trade-off between model accuracy and complexity. An modeling approach that has a high accuracy to predict the stability and dynamic responses of renewable sources also means that this model has higher-order and is more complex. Considering the specific objective of the analysis, an aggregation method that guarantees the model accuracy and computational efficiency can be chosen.

Following an interaction with a vendor, information has been gathered regarding the industrial practices of model aggregation. A comparison of computation time is shown in Table 3. Both inverters and plant controllers can be aggregated. In the majority of case studies, a lumped inverter model ensures sufficient model accuracy. This is especially important from the utility's

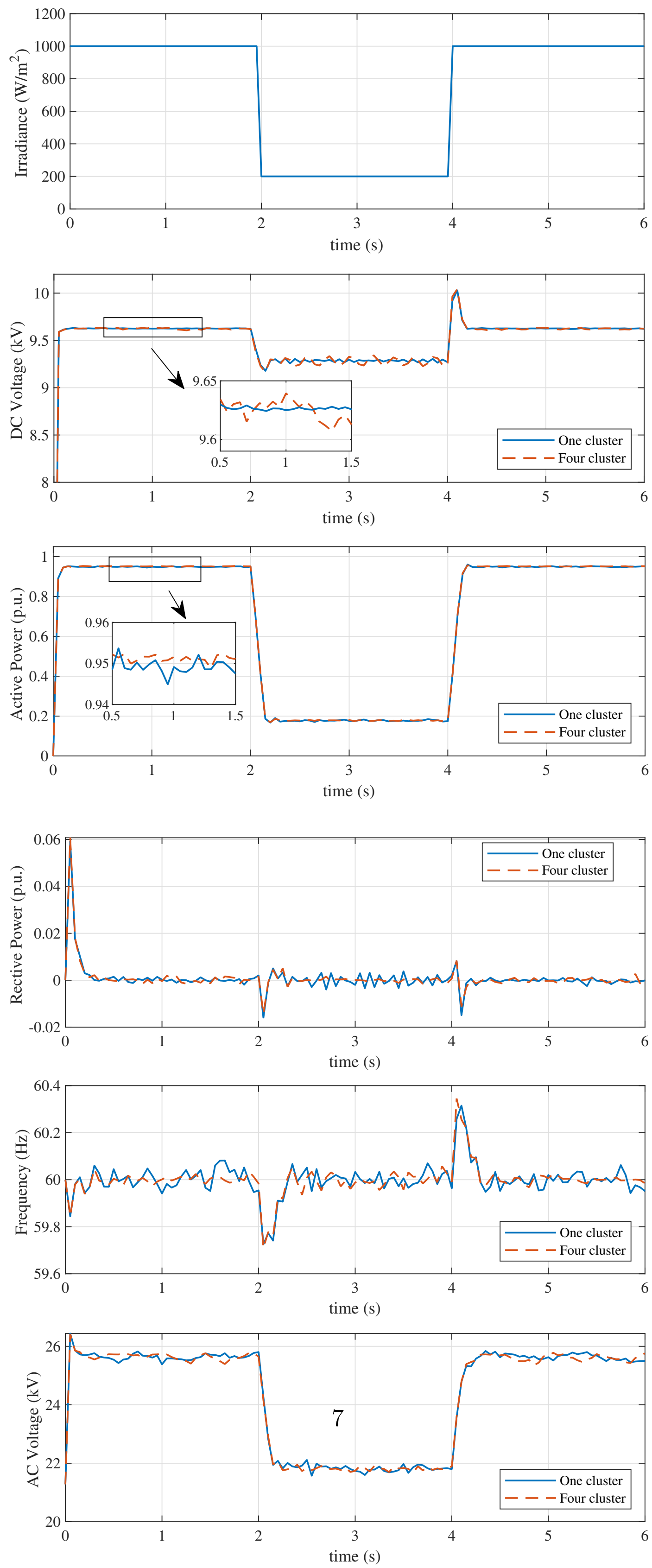

Figure 3: Simulation results under normal operation.

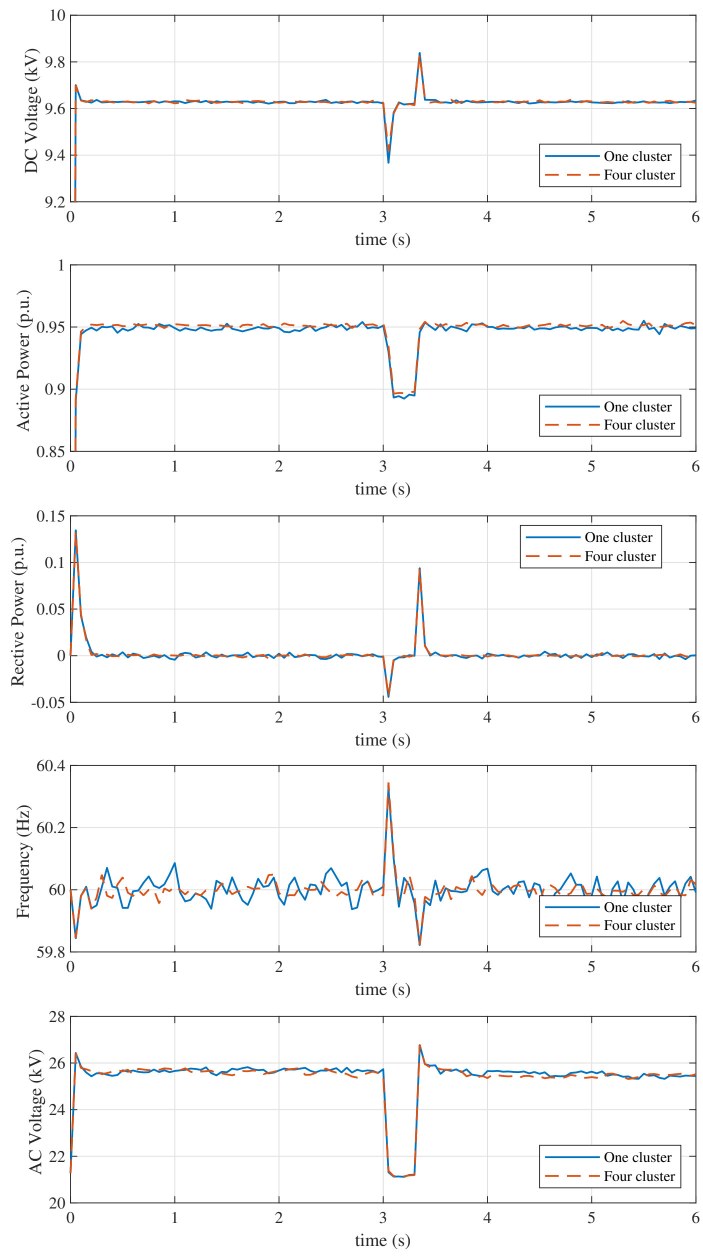

Figure 4: Simulation results under fault condition.

perspective, where computational efficiency and simplicity of models are highly prioritized. However, it should be noted that in the context of offshore wind farms, some variations might occur due to the relatively long internal cables involved.

Test System	Single inverter with simple grid	100 inverters with simple grid	IEEE 39-bus system with 100 inverters and SGs	Real PV plant with 150 inverters	Generic IBR model
Ratio between Simulation Time and Real-Time	1:1.5	1:5	1:100	1:100	1:43

Table 3: Comparison of simulation time.

References

[1] A. A. Kebede, T. Kalogiannis, J. Van Mierlo, and M. Berecibar, "A comprehensive review of stationary energy storage devices for large scale renewable energy sources grid integration," *Renewable and Sustainable Energy Reviews*, vol. 159, p. 112 213, 2022.

[2] N. Hatziargyriou, J. Milanovic, C. Rahmann, *et al.*, "Definition and classification of power system stability – revisited & extended," *IEEE Transactions on Power Systems*, vol. 36, no. 4, pp. 3271–3281, 2021.

[3] M. Martínez-Lavín, R. Villena-Ruiz, A. Honrubia-Escribano, J. C. Hernández, and E. Gómez-Lázaro, "Proposal for an aggregated solar pv power plant simulation model for grid code compliance," *Electric Power Systems Research*, vol. 213, p. 108 676, 2022.

[4] D. Remon, A. M. Cantarellas, and P. Rodriguez, "Equivalent model of large-scale synchronous photovoltaic power plants," *IEEE Transactions on Industry Applications*, vol. 52, no. 6, pp. 5029–5040, 2016.

[5] V. Purba, B. B. Johnson, S. Jafarpour, F. Bullo, and S. V. Dhople, "Dynamic aggregation of grid-tied three-phase inverters," *IEEE Transactions on Power Systems*, vol. 35, no. 2, pp. 1520–1530, 2019.

[6] N. Shabanikia and S. A. Khajehoddin, "Weighted dynamic aggregation modeling of grid-following inverters to analyze renewable dg integrated microgrids," *IEEE Transactions on Industrial Electronics*, 2023.

[7] Simulink. "Simulink documentation." (2023), [Online]. Available: `https://www.mathworks.com/help/simulink/` (visited on 06/03/2023).

[8] "250-kw grid-connected pv array." (2023), [Online]. Available: `https://www.mathworks.com/help/sps/ug/250-kw-grid-connected-pv-array.html` (visited on 08/08/2023).

[9] V. Kaura and V. Blasko, “Operation of a phase locked loop system under distorted utility conditions,” *IEEE Transactions on Industry applications*, vol. 33, no. 1, pp. 58–63, 1997.

[10] B. Subudhi and R. Pradhan, “A comparative study on maximum power point tracking techniques for photovoltaic power systems,” *IEEE transactions on Sustainable Energy*, vol. 4, no. 1, pp. 89–98, 2012.